Aeolian Research 18 (2015) 11–21

Contents lists available at ScienceDirect

Aeolian Research

journal homepage: www.elsevier.com/locate/aeolia

Assessment of a locally-sourced loess system in Europe: The Swiss Jura Mountains

Loraine Martignier [a], Meryl Nussbaumer [a,c], Thierry Adatte [b], Jean-Michel Gobat [c], Eric P. Verrecchia [a,*]

[a] Institute of Earth Surface Dynamics, University of Lausanne, 1015 Lausanne, Switzerland
[b] Institute of Earth Sciences, University of Lausanne, 1015 Lausanne, Switzerland
[c] Institute of Biology, University of Neuchâtel, 2000 Neuchâtel, Switzerland

ARTICLE INFO

Article history:
Received 25 July 2014
Revised 8 May 2015
Accepted 18 May 2015

Keywords:
Loess
Jura Mountains
Grain size distribution
Mineralogy
Geochemical composition

ABSTRACT

Loess of Northern, Central, and Eastern Europe cover large areas and can be of considerable thickness. However, this already well-described loess belt did not reach the Swiss Jura Mountains. Nevertheless, local deflation, transportation, and deposition processes were efficient during the Late Glacial Period. Alpine moraines and outwash deposits on the Swiss foreland worked as deflation sources under the action of winds. Aeolian particles were deposited on the easternmost ridge and summits of the Jura Mountains, forming a thin loessic cover (<50 cm), which was generally eroded and/or incorporated in periglacial sediments. Jura "loess" is enriched in Alpine silicate minerals and constitutes a clear allochthonous input in the context of Jura Mountains, where Mesozoic limestones, and their weathering products, compose the quasi-entirety of autochthonous material. The Jura loess, already recognised for more than 40 years, still needs to be characterised more accurately. Five study sites were chosen along an 85 km long transect on the easternmost ridge of the Jura Mountains. A soil pit was dug and analysed at each site, in order to identify loess layers. Grain-size distribution curves of loess permitted to discriminate four particle subpopulations, which are related to various aeolian episodes/sources and post-depositional weathering processes, respectively. The mineralogical composition is dominated by Alpine components. However, high amounts of kaolinite in the clay fraction of loess layers point to a more local origin, thus indicating the contribution of Jura moraines as potential deflation sources. Finally, the geochemical composition of loess reflects the preponderant influence of Alpine minerals.

1. Introduction

Loess in Northern, Central, and Eastern Europe covers vast areas and constitutes important records of the Quaternary period (Fig. 1; Jamagne, 1973; Lang et al., 2003; Markovic et al., 2006; Preusser and Fiebig, 2009; Zöller et al., 1988 among many others). The Jura Mountains defining the northwestern Franco-Swiss border are not part of this large European loess belt (Frechen et al., 2003; Haase et al., 2007). Nevertheless, thin (<50 cm) and irregularly distributed loess covers the southeastern end of the Jura Mountain range. These deposits, as well as the mixed sediments in which loess is incorporated, form the uppermost layer of superficial deposits commonly observed in the Jura Mountains and constitute the parent material for Holocene soil development (Lorz et al., 2011; Völkel et al., 2001, 2011). Moreover, these aeolian sediments are neither linked to the Po plain loess (Northern Italy), which originated from the reworking of sediments from the Adriatic Sea during Glacial Periods (Cremaschi, 1990). In addition, present-day aeolian inputs, mainly composed of Sahara dust, could only represent a partial and minor contribution to the total amount in loess in the Jura Mountains (Stuut et al., 2009). Jura loess is most likely locally sourced, according to the concept developed by Luehmann et al. (2013) in the Upper Peninsula of Michigan, and the result of nearby aeolian processes, which include deflation, transportation, and deposition of particles on the Jura ridge.

The source area of the Jura loess has been previously described as being composed of Alpine moraines and outwash deposits from the Swiss foreland (Pochon, 1973, 1978), known to be formed by a mix of carbonate and silicate minerals (Portmann, 1954) transported by the Rhône glacier during the Last Glacial Period (from about 114,000–11,000 BP; Ivy-Ochs et al., 2008). Deflation of mineral particles probably started after the glacier melted, during the

* Corresponding author at: Institute of Earth Surface Dynamics, Geopolis – University of Lausanne, CH-1015 Lausanne, Switzerland. Tel.: +41 (0)21 692 44 50; fax: +41 (0)21 692 43 05.
E-mail address: eric.verrecchia@unil.ch (E.P. Verrecchia).

http://dx.doi.org/10.1016/j.aeolia.2015.05.003
1875-9637/

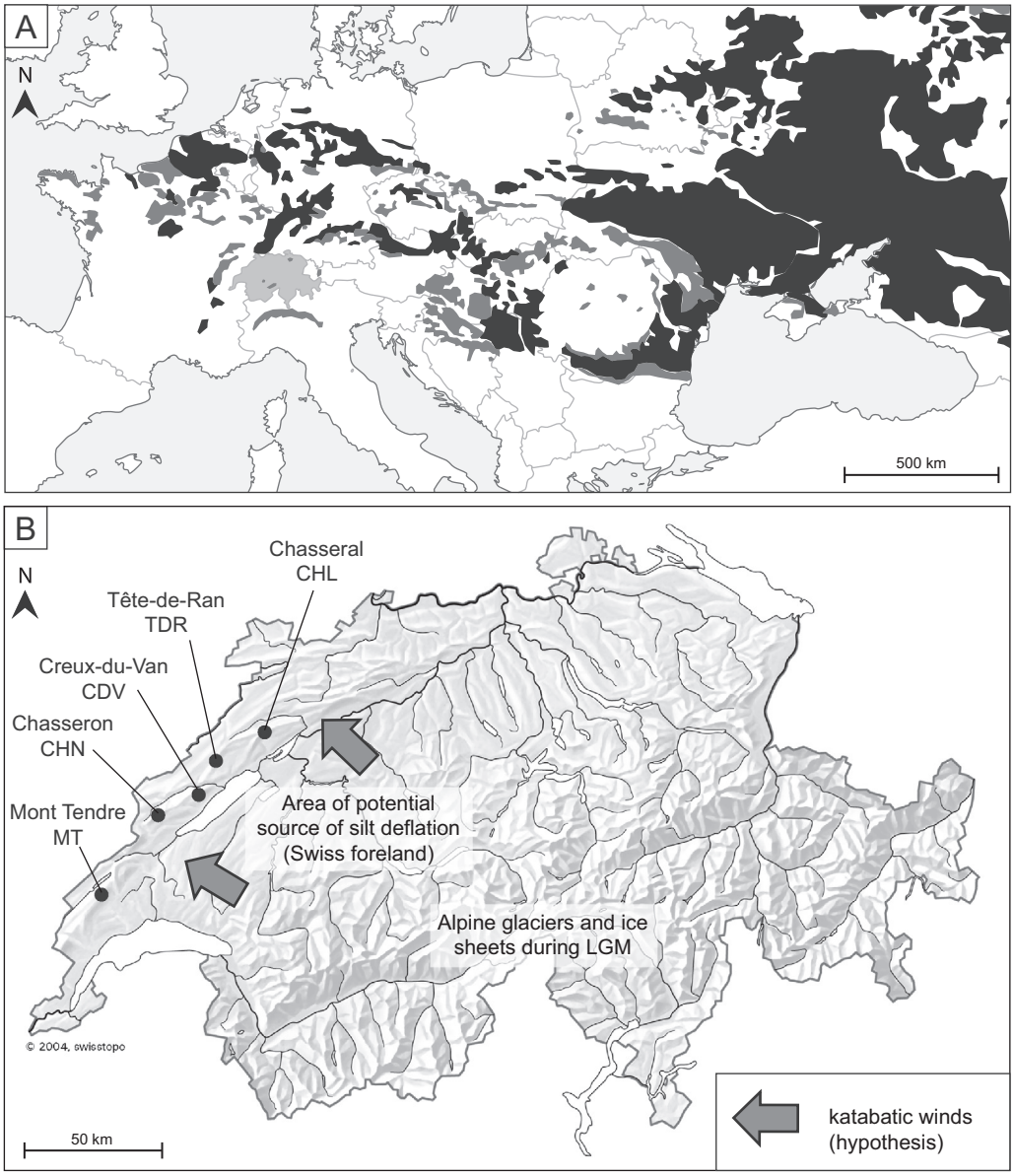

Fig. 1. (A) Location of loess in Europe (redrawn after Haase et al., 2007; Muhs, 2013, and Muhs et al., 2014). Thick loess, thin loess, and sandy loess are indicated in black; "loess derivates" in dark grey. Switzerland is located on the map. (B) Map of Switzerland showing the location of the five study sites and corresponding soil profiles along the first ridge of the Jura Mountains. Potential areas of loess deflation are indicated on the Swiss foreland. The most probable direction of katabatic winds during the LGM is also shown.

Oldest Dryas (from 18,000 to 14,500 BP; Ivy-Ochs et al., 2004). Therefore, it can easily be hypothesised that fine material from the ground moraines was winnowed out by katabatic winds coming from the Alps and descending through the Swiss foreland. The presence of sparse Arctic tundra-like vegetation (Hadorn et al., 2002; Magny et al., 2003) allowed efficient particle deflation (Muhs, 2013). Mineral grains were deposited on the Jura's easternmost ridge to form an approximately 45 cm-thick layer (Aubert et al., 1979), which covered the bare limestone bedrock and the sediments present on summit areas. Loess was preferentially preserved in small depressions and as cladding on the mountain top, as well as in karst features, such as rock cracks (lapiaz) and dolines (Pochon, 1978). However, most of the loess was eroded and redistributed along hill slopes through solifluction and gravity, and integrated in cover-bed deposits (Kleber, 1992; Kleber and Terhorst, 2013; Martignier and Verrecchia, 2013; Martignier et al., 2013). It is hypothesised that loess contained carbonate when they were deposited, according to the composition of their potential source material, but have most likely been decarbonated during early stages of post-glacial pedogenesis, from about 17,000 BP (Magny et al., 2003; Van Vliet-Lanoë, 2005).

The input of Alpine silicate minerals into the calcareous environment of the Jura Mountains has a direct impact on the composition of superficial deposits and therefore, on soil evolution. However, recent studies suggest that there were multiple aeolian episodes, resulting in a mix of distinct subpopulations of grain-sizes, including coarse sand particles (Martignier et al., 2013). Consequently, more proximal deflation sources must also be considered, such as local carbonate moraines situated at the southeastern Jura foot slope (Martignier and Verrecchia, 2013). In the studied context of the Jura Mountains, loess contains loamy particles brought by wind action in a former periglacial environment. This Jura loess must include *in situ* genuine loessic sediments, as well as some slightly reworked loess (corresponding to

"loess derivates"; Haase et al., 2007). The latter displays similar characteristics (i.e., in terms of texture, colour, pH, mineralogy, and geochemistry) to the former.

The first aim of this study is to propose a precise and accurate characterisation of the Jura loess, combining grain-size distribution, mineralogical, and geochemical compositions, and determine the primary characteristics of the Jura loess before reworking and pedogenesis blurred the original signal. Secondly, Jura loess is compared to, and differentiated from, other larger European loess belts and present-day Sahara dust inputs. The Jura Mountains give an opportunity to study locally-sourced loess systems in Europe. Indeed, such local loess is most likely hidden by more important loess complexes, even though locally-sourced systems might exist in many other environments (e.g., in the Vercors massif and the Dolomite Mountains; Gillet et al., 1996; Havlicek, 1999).

2. Study area

2.1. General settings of the Jura Mountains

The Jura Mountains are a 150 km long massif situated at the border of France and Switzerland. Their highest point reaches 1718 m above sea level (a.s.l.). Mainly composed of Mesozoic limestone and marls, the mountain chain has a crescent-like shape, which is due to the formation of the massif subsequently to Alpine orogeny during the Miocene and Pliocene. The inner part (eastern and southern) of the Jura massif is constituted of alternating anticlines and synclines, whereas tabular limestone beds form the outer part (western and northern). As a consequence of erosion, present-day ridges and summits of the inner part are constituted by outcropping hard limestone (e.g., Tithonian, Kimmeridgian, and Sequanian beds). During the Last Glacial Maximum (Last Glacial Maximum – LGM, about 20,000 BP; Ivy-Ochs et al., 2004), the Jura was seemingly covered by a local ice sheet centred on the Joux Valley at the NW of the Mont Tendre summit (Fig. 1; Aubert, 1965). The ice sheet extended southwest and northeast along the Jura massif but did not cover the highest summits (Arn and Campy, 1990). Some ice tongues passed over the first ridge in the southeast and met the Rhône glacier at the Jura foot slope (Aubert, 1965; Campy, 1992). Their point of convergence is situated at an altitude of about 1200 m a.s.l. (Arn and Campy, 1990). As a consequence, the composition of moraine deposits at the southeastern Jura foot slope varies according to the origin of the corresponding glacier: Jura ice sheet moraines contain exclusively carbonate material (rock fragments and fine fraction), whereas Rhône glacier moraines include carbonate and silicate minerals (magmatic, metamorphic, and detrital rocks; Martignier and Verrecchia, 2013). On hill slopes, various types of superficial deposits (cover-beds, colluvium, etc.), mainly reworked by periglacial processes and inherited from the Last Glacial Period, overlie moraine deposits.

Presently, climate in the Jura Mountains is humid and cold temperate with high seasonal temperature contrasts. At the summits (Chasseral, 1607 m a.s.l.), mean annual temperature is 3 °C and mean annual precipitation reaches 1900 mm. Leaching and eluviation processes in soils are enhanced due to a higher precipitation rate than evapotranspiration.

2.2. Description of the study sites

The five study sites are situated on summits of the easternmost ridge of the Jura Mountains along an 85 km long transect oriented NE–SW (Fig. 1). The study sites were not covered by any large ice masses (i.e., Jura ice sheet or Rhône glacier) during the LGM, as no moraine deposits are observed. However, the presence of a snow cover or small local ice cap is likely. Former soils and sediments were eroded due to glacial and periglacial processes and the hard limestone bedrock outcropped at many places. In this context, aeolian particles represent the only possible allochthonous input. Post-depositional reworking of loess was probable at some of the study sites according to the slope, but only a limited mixing with autochthonous material has been possible due to the scarcity of autochthonous weathered material at the time of loess deposition. Consequently, in some places, loessic deposits lay directly on the limestone bedrock and its weathering products (mostly due to frost shattering). In others, some transition layers can be observed in deep soil horizons, at the contact with the bedrock. These transition layers never exceed 40 cm.

The elevation of the study sites ranges from 1406 to 1637 m a.s.l. (Table 1). The Chasseral (CHL), Tête-de-Ran (TDR), Creux-du-Van (CDV), and Mont Tendre (MT) sites are situated on hard limestone bedrock (Oxfordian to Kimmeridgian), whereas the Chasseron site (CHN) lies on an Oxfordian marly bed. At three sites, the slope is fairly steep (about 20°) leading to enhanced erosion of part of the loess cover. All sites are covered by grassland vegetation and used for pasture. They can be put into two categories, depending on the intensity of grazing: an acidic nutrient-poor grassland (*Nardion strictae* Braun-Blanquet 1926) and a nutrient-rich grassland (*Poion alpinae* Oberdorfer 1950).

3. Methods

3.1. Soil description and sampling

A soil profile was dug at each site. The depth of the profiles varied in order to reach the bedrock. Soil horizons were delimited and described according to the World Reference Base WRB (FAO, 2006a). Each horizon was characterised according to its depth, percentage of coarse material (exclusively composed of limestone), texture, structure, and relative abundance of carbonate (tested with 10% hydrochloric acid). Soil profiles were then attributed to a reference soil type (FAO, 2006b). The loessic deposits, the transition layer with the autochthonous material, and the bedrock were identified in each profile, according to the description of soil horizons. Bulk soil was sampled for each horizon in profiles CHL, CDV, and CHN (see Table 1 for abbreviations). In profiles TDR and MT, bulk soil samples were taken in a systematic way (0–5 cm in depth, 5–10 cm, and then every 10 cm until reaching the bedrock). Fragments of limestone bedrock or marls were sampled in each soil profile. Soil samples were dried in an oven at 40 °C for three days and then sieved at 2 mm. Unweathered rock samples were sawn into small pieces and dried. A fraction of each soil and rock sample was crushed in an agate mortar to obtain a powder (grain size < 40 μm). Soil pH was measured in a water solution, with a ratio of 1:2.5 for sieved bulk soil and water, respectively (pH H_2O).

3.2. Analytical methods

In order to perform grain-size analysis, soil and rock samples were treated with 10% HCl to remove the carbonate fraction. Residual material was washed and then treated with 35% hydrogen peroxide in a water bath at 50 °C to remove organic matter. Clay destruction was avoided by a regular pH control (pH 7–8). The reaction was stopped after one week and the excessive hydrogen peroxide was evaporated. A dispersal agent (Na-hexametaphosphate) was added to the samples, which were then shaken during 12 h before analysing. Grain-size measurements were performed using laser diffraction (Malvern Mastersizer 2000, Hydro 2000S module) and the Fraunhofer approximation. Micrometre sizes were converted into Φ values.

Table 1
Main characteristics of the five study sites. Soil type is determined according to FAO (2006b).

Site	Soil profile	Elevation (m.a.s.l.)	Latitudes/longitudes	Exposure	Slope (°)	Geological substrata	Vegetation (alliance)	Soil type
Chasseral	CHL	1570	47°8′N/7°4′E	S	15	Limestone (Kimmeridigian)	*Nardion strictae*	Luvic cambisol
Tête-de-Ran	TDR	1410	47°2′N/6°5′E	SE	<5	Limestone (Kimmeridigian)	*Poion alpinae*	Luvic cambisol
Creux-du-Van	CDV	1406	46°55′N/6°44′E	NW	20	Limestone (Kimmeridigian)	*Nardion strictae*	Cambisol
Chasseron	CHN	1555	46°51′N/6°32′E	SE	20	Marls (Sequanian)	*Nardion strictae*	Cambisol
Mont Tendre	MT	1637	46°35′N/6°18′E	SW	<5	Limestone (Sequanian)	*Poion alpinae*	Luvic cambisol

Finally, the average distribution curve of Jura loess was deconvolved using PeakFit™ (Systat Software Inc.) with a Gaussian operator, in order to discriminate the different particle modes composing the total curve and determine their relative abundance.

The mineralogical composition was determined using X-ray diffraction (XRD) on the bulk, fine silt (2–16 μm), and clay (<2 μm) fractions of soil and rock samples (Adatte et al., 1996), using an ARL Xtra diffractometer (Thermo). The bulk composition was measured on the sample powder compressed in holders. The peak intensities of recognised major minerals were converted into relative abundances, according to external standards. Organic matter and amorphous or poorly crystallized minerals (i.e., various iron oxides and phyllosilicates) are included in the non-quantified fraction. For the fine silt and clay fractions, 2 mm-sieved soil samples and limestone rock cuttings were treated with 10% HCl in an ultra-sonic bath for 3 min in order to remove carbonate. Both fractions were separated by centrifugation and deposited on distinct glass plates. Samples were glycolated before XRD analysis to detect swelling clay minerals. For the <2 μm fraction, the part of the diffractogram corresponding to the various interlayered clay minerals was treated using PeakFit™ (Systat Software Inc.). The 4–11°2θ section was smoothed by a Fourier transform function and deconvolved using the Pearson VII operator. This procedure allows poorly crystallized clay minerals resulting from weathering processes in soil to be discriminated, i.e., interlayered illite–vermiculite (IV), hydroxy-Al–Fe intergrade illite–vermiculite (IV–Al–Fe, corresponding to hydroxy interlayered vermiculites or HIV; Velde and Meunier, 2008), smectite, and interlayered illite–smectite (IS). Well-crystallized phyllosilicates, such as mica, kaolinite, and chlorite, are identified according to the position of their peak on the diffractogram. Relative abundance for each clay mineral is calculated with its respective peak intensity. Results are given in counts per second (cps) for other detected minerals (e.g., Na-plagioclase and K-feldspar).

The bulk chemical composition of soil and rock samples was measured with X-ray fluorescence (XRF), using a FRX Philips PW2400 spectrometer. The powder of each sample was compressed and dried at 105 °C before analyses. Results were calculated in percentage of major and trace elements and then corrected using the loss on ignition value at 1050 °C.

4. Results and discussion

4.1. Description of the sediment layer

The five described soil profiles belong to Cambisol or Luvic Cambisol references (Table 1). All soil profiles present a thin surficial A horizon (2–5 cm thick), where humified organic matter is mixed with the mineral fraction (FAO, 2006a). The loess layers are between 50 and 95 cm thick and situated at the surface (Table 2). Surface horizons of these layers are devoid of coarse material (>2 mm). But this coarse fraction increases up to 90% in deeper horizons of loess layers and is exclusively composed of limestone fragments. In such fragment-rich horizons, loess particles accumulate in between large limestone fragments, thus filling cracks and pores. However, it has been observed that the loessic material itself is not mixed with autochthonous components. Consequently, the fine fraction of these horizons (<2 mm) is mainly composed of homogeneous aeolian particles and therefore is included in the "loess layer". The soil texture is dominantly silt loam, with a clay fraction increasing with depth. Horizons are non- or weakly calcareous in loess layers. pH values are slightly acidic (the lowest value is 5.3 in profile CDV) and display an increasing trend towards deep horizons of the loess layer (up to 8.3 in profile CDV and CHL). The thickness of transition layers, where loess particles are mixed with autochthonous material within the soil fine fraction (<2 mm), varies between 10 cm (soil

Table 2
Description of loess layers, transitions layers, and bedrock in each soil profile according to FAO (2006a) descriptive codes.

Soil profile	Sediment layer	Depth (cm)	No. of samples	% coarse (limestone)	Texture[a]	% $CaCo_3$[b]	pH H_2O
CHL	Loess	0–94	5	0–70	SiL–SiCL	0–10	5.6–8.3
	Transition layer	94–121	1	90	C	2–10	8.5
	Bedrock (limestone)	>121	1			>25	
TDR	Loess	0–50	6	0–20	SiL–SiC	0	5.9–7.3
	Transition layer	50–60	1	90	SiC	0	7.8
	Bedrock (limestone)	>60	1			>25	
CDV	Loess	0–84	6	0–90	SiL–SiCL	0–25	5.3–8.3
	Transition layer	84–100	1	90	C	10–25	8.4
	Bedrock (limestone)	>100	1			>25	
CHN	Loess	0–63	4	0–70	SiL–C	0–2	5.9–7.4
	Transition layer	63–105	1	95	C	>25	8.7
	Bedrock (marls)	>105	1			>25	
MT	Loess	0–50	6	0–50	SiL–SiCL	0	5.6–6.9
	Transition layer	50–60	1	90	SiC	0–2	7.8
	Bedrock (limestone)	>60	1			>25	

[a] C = clay; SiC = silty clay; SiL = silt loam; SiC = silty clay loam.
[b] Carbonate reaction to HCl 10%, estimation of carbonate content.

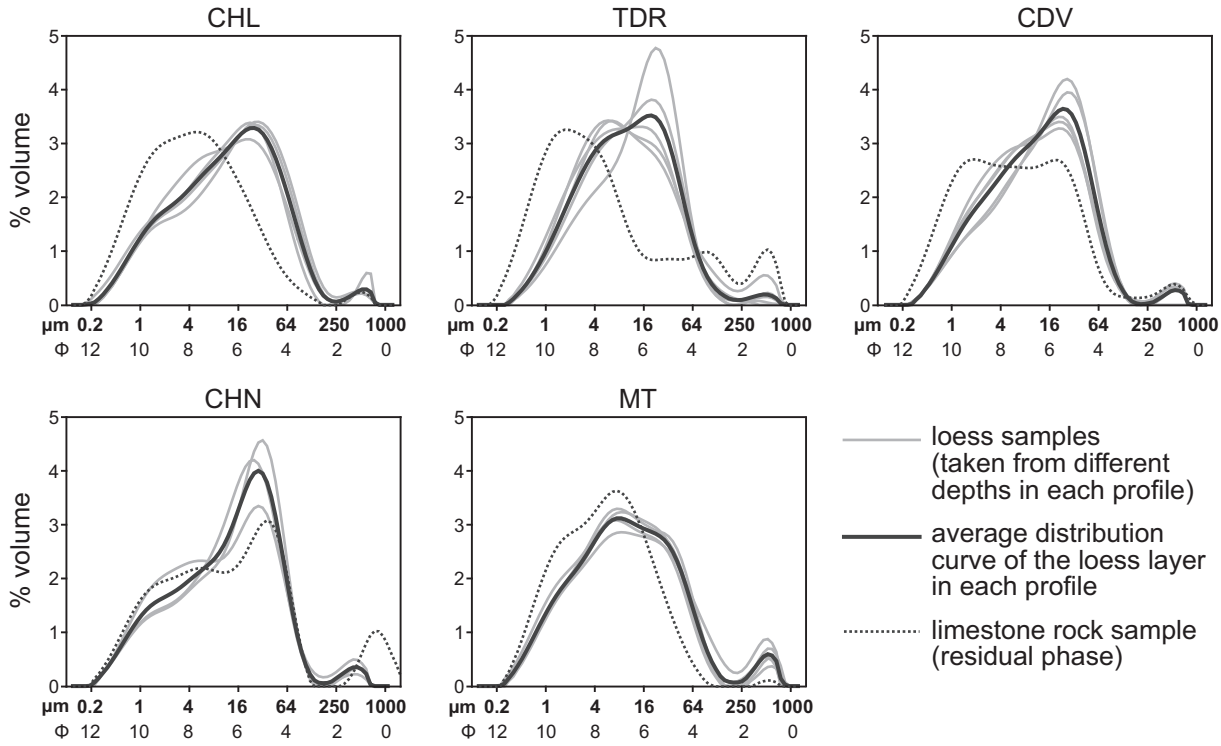

Fig. 2. Grain-size distribution curves of loess and bedrock samples (weathering residue; dotted lines). Individual loess-sample distributions are shown in grey (samples were taken at different depths along the soil profile). The average distribution curve of the loess layer is given for each profile (in black). Uppermost samples of each profile are not included.

profiles TDR and MT situated on hard limestone) and 42 cm (soil profile CHN situated on marls). Compared to the surface loess layers, transition layers are characterised by a higher content in coarse material (limestone fragments) and a more clayey texture. The calcite content is similar to or higher than in the loess layer and pH values are alkaline (between 7.8 and 8.7). Finally, rock fragments, sampled in the deepest horizon of soil profiles, are composed of hard limestone or marls and present an evident high calcite content.

4.2. Grain-size distribution

Analytical results emphasise the main characteristics of Jura loess. The uppermost sample of each profile (corresponding to the A horizon) is not taken into account, in order to minimise the influence of organic matter dynamics on the composition of the mineral particles of soils. As a comparison, bedrock data are displayed using the mean of five sampled limestones and marls. Results on transition layers, where loess is mixed with weathered autochthonous material at various degrees, are not presented here but are accessible in a complete data set available in additional material.

Grain-size curves of loess layer samples show similar distributions within each soil profile (Fig. 2). In profiles CHL, CDV, and CHN, the main grain-size mode is between 16 and 32 μm (corresponding to 6 and 5 Φ, respectively) with a secondary mode around 4–8 μm (8–7 Φ). This second mode is more represented in some samples of profile TDR, thus influencing the mean distribution curve of this particular loess layer. However, the 4–8 μm is dominant in soil profile MT and the 16–32 μm mode becomes of secondary importance. In all profiles, a clay subpopulation (1–2 μm; 10–9 Φ) is detected, as well as a discreet coarse sand subpopulation (500 μm; 1 Φ). The residual phase of bedrocks shows various distribution patterns according to the samples, but presents higher clay content than loess layer samples, in general. In soil profiles CHL and TDR, the distribution curves from rock samples strongly differ from those of the overlying loess layers. In other soil profiles, some similarities can be observed (grain-size modes at 16–32, 4–8, or 500 μm), but the correspondence between loess and rock samples is never complete. Deconvolution of the average grain-size distribution of loess layers (average of the five profile means) allows four main particle subpopulations to be identified, which are characterised by their respective mode and contribution (Fig. 3). The dominant grain-size mode corresponds to coarse silt (30 μm; 5.1 Φ) and represents 45% of the total average loess composition. A secondary mode of fine silt (6 μm; 7.5 Φ) stands for 39% of this total. The remaining particles are distributed in clay (1.2 μm; 9.7 Φ) and coarse sand (500 μm; 1 Φ) modes.

4.3. Mineralogical and geochemical results

The average bulk mineralogical composition of the loess layers is carbonate-free and contains up to 48% quartz and 33% phyllosilicates (Fig. 4). Plagioclase and feldspar are present in various amounts according to the profiles (between 2–4% and 3–10%, respectively) and goethite is identified in small proportions in profiles CHL and MT. The non-quantified fraction represents up to 19% of the bulk composition. In contrast to the loess layers, the average bedrock composition is predominantly composed of calcite (99%), accompanied by a scarce non-quantified fraction. The fine silt fraction (2–16 μm) is characterised by the presence of mica, kaolinite, and chlorite, and specific Na-plagioclase/K-feldspar ratios (pla/FK ratio). In the loess layers, chlorite represents from 40% to 60% of the three phyllosilicate minerals, whereas mica remains in a constant proportion of about 30%. The pla/FK ratio displays values between 0.90 and 1.80 for loess layers, which indicates that Na-plagioclase is present in proportions fairly similar to K-feldspar, except in soil profile CDV, where Na-plagioclase is

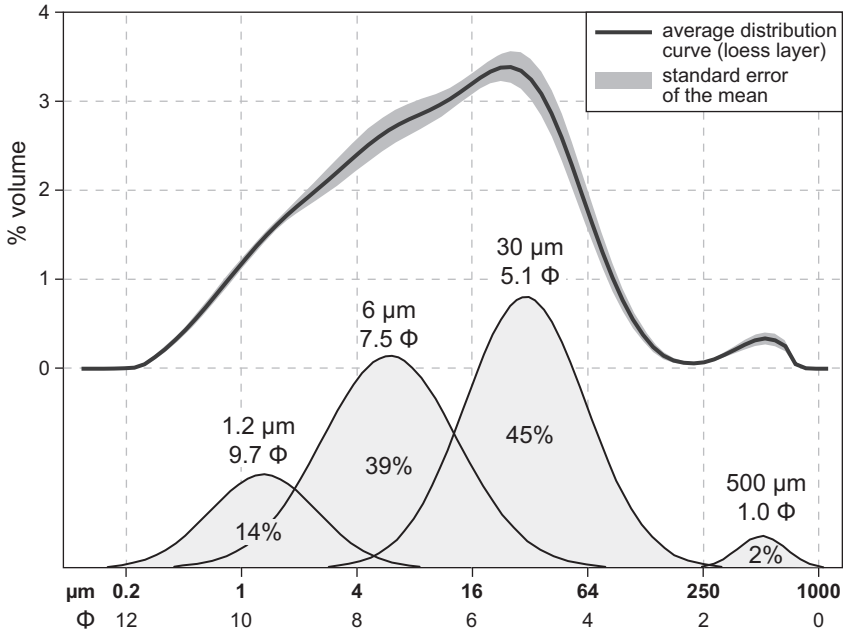

Fig. 3. Average grain-size distribution for Jura loess (average of the five loess layer means) and standard error of the mean. The average distribution curve is deconvolved using PeakFit™ (Systat Software Inc.) with a Gaussian operator. Four particle subpopulations are identified by their respective mode and contribution to the total average curve (% distribution function area).

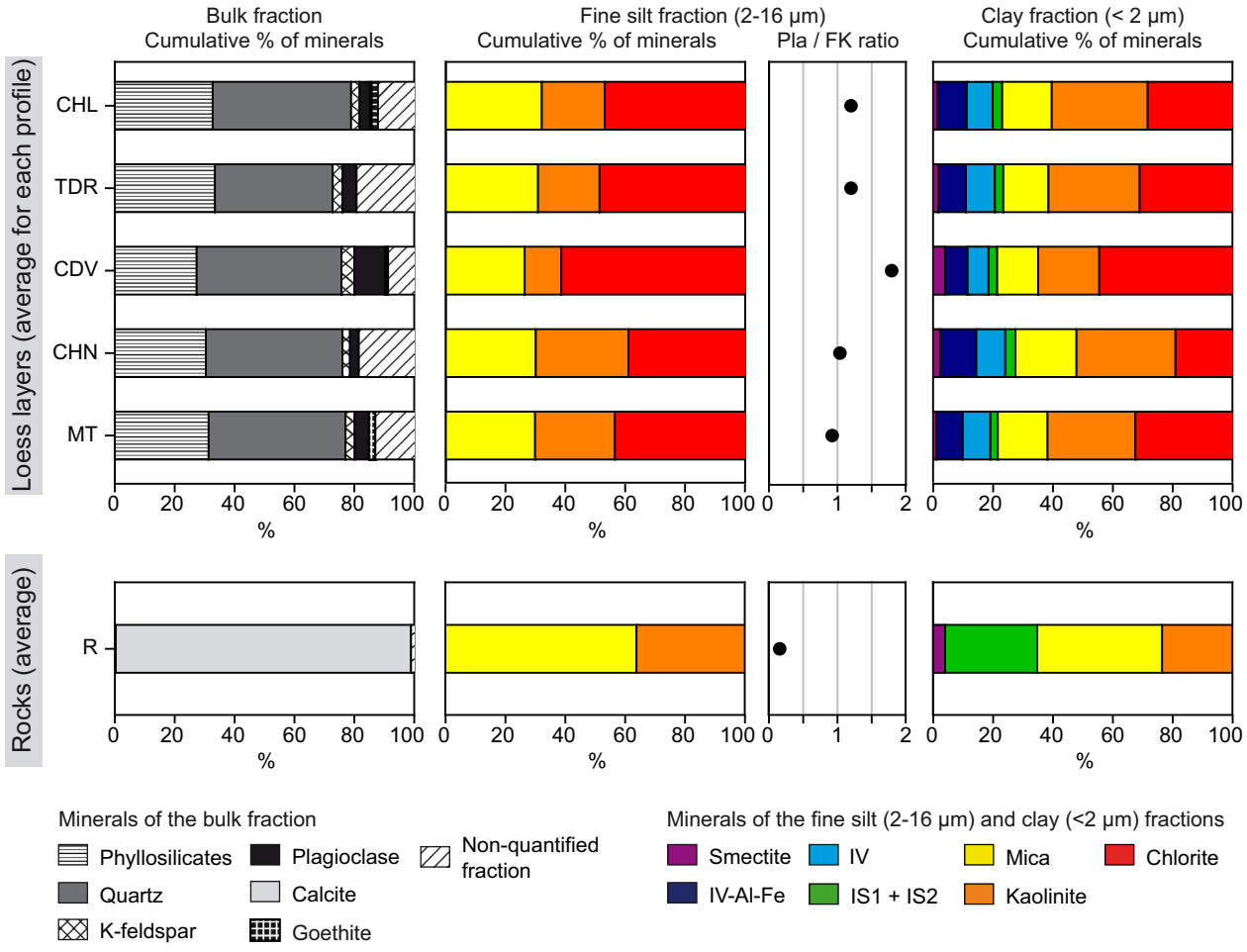

Fig. 4. Mineralogical composition of bulk and non-carbonate fine silt (2–16 µm), and clay (<2 µm) fractions of loess layers given as an average of each soil profile (without the first surficial horizon in each profile). As a comparison, the average mineralogical composition of limestone bedrocks is given.

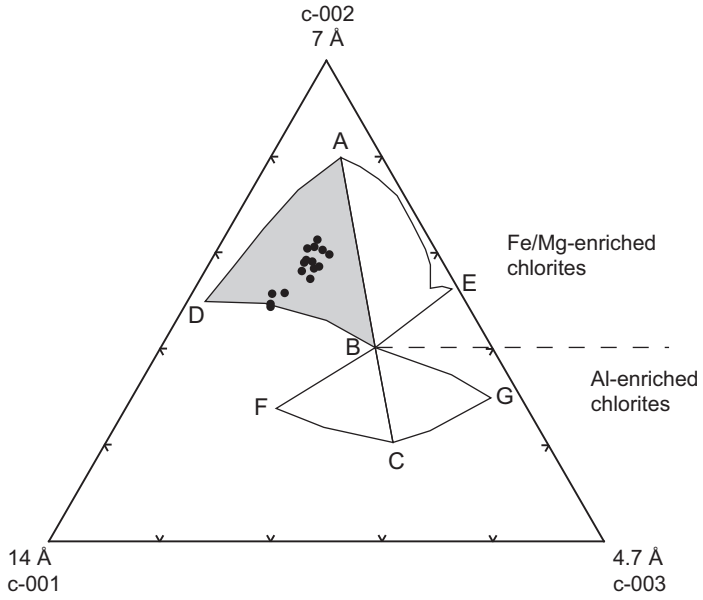

Fig. 5. Ternary diagram showing the chlorite type of the 2–16 μm fraction of loess samples. The ABD area corresponds to chlorite containing high amounts of iron in silicate layers (Oinuma et al., 1972).

significantly more abundant than K-feldspar. Small amounts of amphibole are detected in some samples of the 2–16 μm fraction of loess layers, but are not quantified (not shown in the figure). Finally, chlorite is absent in the fine silt fraction of bedrocks, where mica dominates kaolinite and the low pla/FK ratio (average value of 0.16) indicates the predominance of K-feldspar on Na-plagioclase in the non-carbonate fraction of bedrock. Chlorite minerals detected in the 2–16 μm fraction of loess are identified as iron-rich types, according to their XRD diffraction pattern (Fig. 5; Oinuma et al., 1972). Regarding clay mineralogy, chlorite and kaolinite compose the main part of the <2 μm fraction of loess layers (up to 45% and 33%, respectively). Mica and weathering products (such as IV and IV–Al–Fe) are also present, as well as small amounts of interlayered illite–smectite (IS1 and IS2) and smectite. In the bedrock, mica (42%), IS (31%), kaolinite (23%), and smectite (4%) constitute the <2 μm clay fraction.

The average bulk geochemical composition of loess layers shows similar values for Si, Ca, Mg, K, Al, Ti, and Sr for the five profiles, whereas Fe and Mn vary slightly between sites (Fig. 6). Compared to the bedrock's average composition, loess layers are

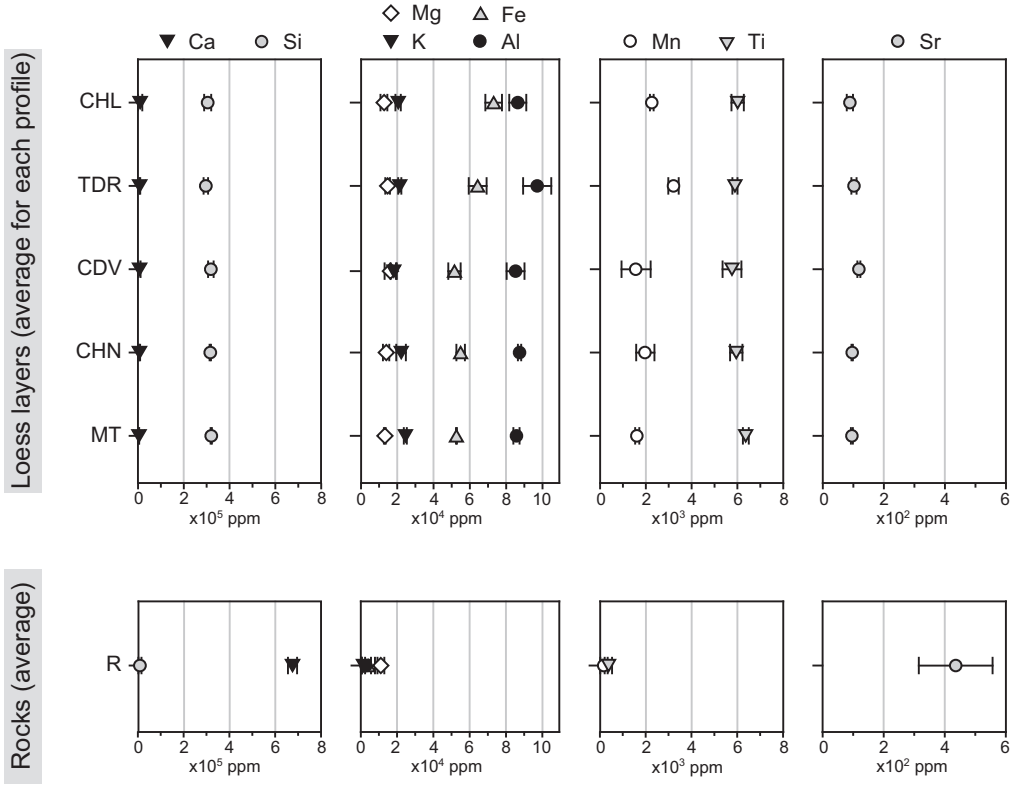

Fig. 6. Average bulk geochemical composition of loess layers for each soil profile (without the first surficial horizon in each profile) and limestone bedrocks.

strongly enriched in Si (>300,000 ppm), Al (up to 99,000 ppm in TDR profile), Fe (up to 73,000 ppm in CHL profile), and Ti (<6000 ppm). In contrast, Ca and Sr are impoverished in loess layers as expected. Carbonate bedrocks contain up to 700,000 ppm of Ca and 560 ppm of Sr.

5. Discussion

5.1. Main characteristics of the Jura loess

According to the first complete description of Jura loess (Pochon, 1978), some grain-size and geochemical characteristics can be now amended, whereas mineralogical results of the present study are in accordance with former results. The technique used to measure grain-size distribution (i.e., laser diffraction) generates difficulties for new data comparison with former results obtained with sieving-pipette methods (Di Stefano et al., 2010). Laser-diffraction measurements produce more detailed results than the sieving-pipette method, allowing dominant particle populations to be discriminated, rather than proportions of particles belonging to delimited grain-size classes. In the present study, an average textural signature is proposed for the Jura loess. Four main grain-size modes are discriminated (potential origin is discussed below), with a dominance of coarse and fine loam (modes at 30 and 6 μm, respectively; Fig. 3). In contrast, the weathering residue of bedrocks contains abundant very fine loam (<4 μm) and clay phases. Taken as a whole, these results correspond to those obtained by Pochon (1978), who noted that the dominant fraction in loess was 16–32 μm and, in limestone bedrock residue, 2–6 μm.

Regarding the bulk and clay-mineralogical compositions, important differences are observed between loess layers and underlying limestone bedrock (Table 3). In the bulk fraction of loess, quartz, phyllosilicates, plagioclase, and feldspar represent 45%, 31%, 6%, and 3% on average, respectively, whereas these minerals are not detected in the analysed bedrocks, or only as traces (e.g., quartz < 1%). The loess layer contains <1% calcite. However, primary loess might have contained some carbonate, as their deflation sources (i.e., Alpine moraines of the Swiss foreland) contain large amounts of limestone sediments in the <2 mm fraction (Guenat, 1987; Portmann, 1954). Decarbonation was probably efficient after loess deposition on the Jura ridge, due to the loamy texture of aeolian particles and to climatic conditions, which enhanced leaching processes (Van Vliet-Lanoë, 2005). The average mineralogical composition of loess clay fraction is constituted by iron-rich chlorite (32%), kaolinite (28%), mica (16%), interstratified weathering products (IV and IV–Al–Fe; 18% in total), and small proportions of smectite and IS (5% in total). The bulk and clay-mineralogical results are in accordance with former data, which emphasise the abundance of quartz and phyllosilicates in the bulk fraction, as well as the dominance of Na-plagioclase on K-feldspar (Pochon, 1978), also observed in the fine silt (2–16 μm) fraction of the loess layers. In the clay fraction, Pochon (1978) measured less chlorite (17%) and more mica (23%) and interstratified weathering products (24%) compared to the present study. Kaolinite (30%), smectite and IS (6% in total) content are similar in both studies. The scarce presence of amphibole in the 2–16 μm fraction of loess layers also emphasises the Alpine origin of the aeolian sediments in the Jura soils, as it is not found in the limestone bedrocks.

The bulk geochemical composition shows a sharp boundary between loess layers and bedrocks, and reflects their respective mineralogical contents and origins. Si, Al, Fe, K, Mn, and Ti are dominant in loess (Table 3) and related to allochthonous silicate minerals. On the other hand, Ca and Sr are abundant in bedrocks constituted by Jurassic marine limestones. Loess is particularly enriched in Fe and Ti compared to Alpine moraines of the south-eastern Jura foot slope (Martignier and Verrecchia, 2013), thus suggesting a preferential selection of loess mineral components enriched in both elements during aeolian deflation. The average geochemical composition of loess layers in the five soil profiles is very similar, thus highlighting the remarkable homogeneity of aeolian sediments in the Jura Mountains, despite of the small variations observed in the mineralogical composition. Pochon (1978) did not measure the bulk geochemical composition in loess, but it represents a pertinent tool to identify loess contributions in soils, even in the case of weak allochthonous inputs mixed with autochthonous material (Martignier, 2013).

5.2. Contribution of distinct particle subpopulations to loess layers

The four distinct grain subpopulations identified on the average grain-size curve of loess highlight the possible contribution of multiple aeolian episodes and/or deflation sources, coupled with post-depositional pedogenic processes (Vandenberghe, 2013). Subpopulations characterised by coarse (30 μm) and fine (6 μm) silt modes together represent about 85% volume of the loess layer. These fractions are responsible for the main mineralogical and geochemical characteristics of loess layer samples. The presence of bimodal loess suggests the involvement of various aeolian episodes/sources that are probably linked to changes in paleoenvironmental conditions during loess deposition (Stanley and Schaetzl, 2011; Schaetzl and Attig, 2013). In addition,

Table 3
Mean mineralogical (bulk and clay fraction) and bulk geochemical composition of Jura loess and limestone bedrocks.

	Phyllosilicates	Quartz	K-feldspar	Plagioclase	Calcite	Geothite	Non-qualified
Bulk mineralogy (%)							
Loess sample (n = 22)	30.9 ± 4.9	45.1 ± 5.9	3.3 ± 1.7	6.2 ± 4.5	0.2 ± 0.6	1.1 ± 1.8	13.2 ± 8.3
Limestone rocks (n = 5)	0.0 ± 0.0	0.3 ± 0.7	0.0 ± 0.0	0.0 ± 0.0	98.6 ± 0.5	0.0 ± 0.0	1.0 ± 0.5
	Smectite	IV–Al–Fe	IV	IS1 + IS2	Mica	Kaolinite	Chlorite
Clay mineralogy <2 μm (%)							
Loess sample (n = 22)	2.2 ± 1.4	9.1 ± 3.3	8.7 ± 2.3	3.0 ± 0.9	16.4 ± 5.2	28.3 ± 7.4	32.3 ± 10.5
Limestone rocks (n = 5)	4.1 ± 2.5	0.0 ± 0.0	0.0 ± 0.0	30.7 ± 10.2	41.7 ± 8.1	23.2 ± 15.6	0.3 ± 0.6
	Ca	Si		Al	Fe		Mg
Bulk chemical composition (mg/kg)							
Loess sample (n = 22)	7286 ± 4706	310,945 ± 13,195		88,489 ± 6543	59,070 ± 8951		14,261 ± 2175
Limestone rocks (n = 5)	674,870 ± 19,887	9281 ± 6801		3093 ± 2518	4071 ± 3757		11,051 ± 1893
	K	Mn		Ti	Sr		
Loess sample (n = 22)	21,316 ± 2623	2140 ± 722		5996 ± 321	102 ± 12		
Limestone rocks (n = 5)	1465 ± 937	179 ± 160		370 ± 161	436 ± 121		

present-day Sahara dust could possibly contribute to the fine silt mode, as its mineralogical composition is similar to Alpine loess (quartz, calcite, dolomite, and mica; Kübler et al., 1990). There is more coarse silt than fine silt in all studied soil profiles, except for the Mont Tendre site (MT), which is the most southeastern site. These grain-size distributions could have been caused by variations in intensity and direction of winds. It seems reasonable to consider that katabatic winds descending from the Alps at the end of the Last Glacial Period contributed to this particle redistribution, as these winds are currently considered as very efficient in loess transportation (Muhs and Budahn, 2006; Schaetzl and Attig, 2013). But the influence of regional and synoptic winds cannot be discarded, mostly along the Swiss foreland.

The grain subpopulation around the coarse sand mode (500 μm) represents only 2% of the average grain-size curve of loess, but is detected in all studied profiles, mainly in surface samples. The residue of some analysed limestone bedrocks also comprises coarse sands, which could be released during dissolution of limestone bedrocks and outcrops and integrated into the soil profile. Nevertheless, this mixing with bedrock sands due to pedogenic processes is conceivable in thin loess layers (<50 cm) such as in TDR or MT profiles, but might not be effective in thicker profiles (Luehmann et al., 2013; Schaetzl and Luehmann, 2013). However, the weathering residue of TDR and MT hard limestone represents <2% of the total bedrock weight, which is not sufficient to provide enough sandy material to the soil profile, as also observed by Schaetzl and Attig (2013) in similar loess settings. The CHN profile is developing on a marly bed, which could release more weathering residue during dissolution. Sand grains were measured in the residue of CHN marls, but they are characterised by an even coarser mode (1000 μm; 0 Φ) than the one observed in the overlying loess layer. Quartz sand grains coming from a surficial cover-bed of a nearby site in the Jura Mountains were observed with a scanning electron microscope (SEM; Martignier et al., 2013). V-shaped percussion marks were identified on the edges of rounded grains, indicating wind transportation. These observations suggest that at least a part of the sand population could have been brought by aeolian transportation. According to the large size of the grains, more proximal deflation sources than the moraines from the Swiss foreland must be considered. Therefore, it is proposed that the mixed-till deposits lying at the southeastern Jura foot slope could have acted as deflation sources during strong wind episodes (i.e., storms; Antoine et al., 2002; Martignier et al., 2013).

Finally, the population around the clay mode (1.2 μm) probably results from *in situ* weathering and disaggregation of loamy particles in soils, in particular as a consequence of decarbonation of loess layers after deposition. The mineralogical composition of the <2 μm fraction contains both allochthonous (mainly chlorite) and autochthonous (mainly kaolinite) minerals. The double origin of the clay fraction might reflect the contribution of Alpine and local deflation sources of loess (Martignier et al., 2013). The contribution of Sahara dust as admixture to the soil is also possible (Kübler et al., 1990; Stuut et al., 2009). Moreover, a low input of *in situ* weathered material is possible through bioturbation, although results above show that loess layers are well differentiated from autochthonous materials.

5.3. Comparison of the five studied profiles

The loess layers studied in the five soil profiles display very similar grain-size, mineralogical, and geochemical compositions. However, some differences can be highlighted. Concerning the grain-size distribution patterns, the main modes are situated at 30 and 6 μm in all sites. The 30 μm is dominant over the 6 μm in four profiles (CHL, TDR, CDV, CHN), whereas it is the opposite in the MT profile. The MT site is situated at the southwestern end of the studied transect. Its special mode distribution might result from the effect of the geographical location, linked with the paleocirculation of winds at the time of loess deflation, transport, and sedimentation. The average bulk mineralogical composition of each profile shows variations within the proportion of the non-quantified fraction. These variations can be related to Holocene pedogenic and weathering processes, as this fraction is mainly composed of organic matter, poorly crystallized iron oxides, and weathered clay minerals. Small differences between the five profiles are observed in plagioclase (bulk fraction) and chlorite (clay fraction) contents. These differences could reflect the mineralogical heterogeneity, which existed locally between the loess deflation sources (i.e., the Alpine moraines on the Swiss foreland), as well as the irregular mixing with more local loess sources (i.e., mixed Alpine and Jura moraines at the southeastern Jura foot slope). Finally, some small variations in Al, Fe, and Mn contents are observed in the average geochemical composition of the five studied profiles. The variation in Al proportion might be due to the slight differences in the mineralogical composition of loess. However, Al can be mobile under specific soil conditions, which induce processes such as clay weathering, acidification, cheluviation, etc. (Duchaufour, 1983; Righi et al., 1999). Therefore, variations in Al between soil profiles can likely be attributed to either variations of primary loess composition, or post-depositional pedogenesis. The same hypothesis can be applied to the slight differences in the Fe and Mn contents between the studied profiles, as both elements are easily redistributed in soil according to efficient soil processes (brunification, clay leaching, redoxic conditions, etc.; Gratier and Bardet, 1980; Martignier, 2013; Schaetzl and Anderson, 2005).

5.4. Context of loess deposition in the Jura Mountains

Loess deposition on the Jura ridges took place at the end of the Last Glaciation, when Alpine moraines and outwash deposits of the Swiss foreland and the southeastern Jura foot slope were exposed to wind deflation (Pochon, 1973, 1978). The incorporation of loessic particles in a late-formed moraine of a local Jura glacier indicates that aeolian transportation was already efficient during the early withdrawal stages (Pochon, 1978). Moreover, Alpine loess is incorporated in periglacial cover-beds described on the Jura foot slope (Martignier and Verrecchia, 2013; Martignier et al., 2013). These sediments were seemingly soliflucted during the Younger Dryas (12,600–11,500 BP; Mailänder and Veit, 2001; Terhorst, 2007; Terhorst et al., 2009). As a consequence, loess deposition on the Jura ridges might have occurred between the LGM (about 20,000 BP; Ivy-Ochs et al., 2004) and the Younger Dryas.

Presently, loess constitutes slightly acidic sediments and leads to brunification and sometimes clay leaching processes in soils (Havlicek, 1999; Martignier and Verrecchia, 2013; Michalet, 1982). However, because of the thinness of the loess layer, which is generally lying on carbonate materials (bedrock or local weathering products), calcium uptake is possible through bioturbation processes (earthworms, roots), thus preventing a stronger acidification (Havlicek and Gobat, 1996; Havlicek et al., 1998).

5.5. Comparison with European loess and present-day Sahara dust

The large loess systems described in Northern, Central, and Eastern Europe were active intermittently throughout the Pleistocene. Their deposition was mainly influenced by the modification of atmospheric circulation due to millennial climatic variations in the North Atlantic and Greenland (Florineth and Schlüchter, 2000; Rousseau et al., 2002). However, there were numerous sources of deflation, which led to various loess, differing in mineralogical composition. As a result, loess in Europe is far

from homogeneous (Antoine et al., 2001; Frechen et al., 2003). The youngest loess in France, Belgium, and South Germany is from the Upper Pleniglacial and is composed of thick and calcareous layers (Antoine et al., 2001; Frechen et al., 2003; Jamagne, 1973). The non-carbonate fraction is dominated by quartz accompanied by low proportions of feldspar, muscovite, and biotite, whereas the clay mineralogy is mainly composed of smectite, vermiculite and illite (Lautridou, 1984). The grain-size distribution of loess usually stands between 10 and 50 μm (Lautridou, 1984). However, a population of fine sands (50–200 μm) can be abundant due to the action of strong winds, which rework local sediments (e.g., in the Rhein valley; Antoine et al., 2001). Therefore, a precise comparison of the Jura loess to other European loess is fairly difficult to establish. Nevertheless, the high chlorite (32% in average) and kaolinite (28% in average) contents in the Jura loess distinguish them from large European loess systems. Concerning the grain-size distribution, the Jura loess presents two prevailing modes situated at 6 and 30 μm, respectively. Such modes are in agreement with other European loess, as well as with typical loess or clayey loess definitions (Haase et al., 2007; Pye, 1987).

Loessic deposits in northern Italy are mostly homogeneous and present a low carbonate content (>5%; Cremaschi, 1990), high plagioclase and muscovite proportions, as well as moderate amounts of quartz (Ferraro et al., 2004). The clay mineralogy is dominated by well-crystallized illite (46–70%), accompanied by chlorite (21–37%), interlayered illite–smectite (6–13%), and kaolinite in very small amounts (2–6%; Ferraro et al., 2004). The grain-size distribution displays median values between 6 and 32 μm and includes various proportions of sand (1–5%) and clay fractions (5–40%; Cremaschi, 1990). The northern Italy loess is distributed on the margin of the Po plain and in the Italian Pre-Alps and is not described in northern areas (e.g., in the Swiss Alps; Cremaschi, 1990). They present some similarities with the Jura loess (plagioclase and chlorite contents, grain-size modes), but no connection between both systems is considered, according to the geographical extent of the Northern Italy loess belt.

Finally, Sahara dust collected at the Jura foot slope (Neuchâtel) in 1989 displayed four distinct grain-size modes at 4,5, 15–20, 40–50, and <2 μm (modes given according to their decreasing contribution to the total grain-size distribution; Kübler et al., 1990). Therefore, the possible contribution of Sahara dust as an admixture to soils might only interfere with the fine silt and clay modes of Jura loess, as the 15–20 and 40–50 μm modes of Sahara dust were not measured in the loess. The bulk mineralogical composition of Sahara dust contained quartz, calcite, dolomite, and mica (Kübler et al., 1990). Na-plagioclase, K-feldspar, kaolinite, and chlorite were also detected in small amounts. This bulk mineralogy is similar to the composition of the Alpine loess and might cause difficulties for the discrimination of both deposits. However, present-day Sahara dust inputs in Switzerland are not sufficient to form distinct sediments layers, but rather represent admixtures to soils (Stuut et al., 2009).

6. Conclusions

The Jura loess constitutes a locally-sourced loess system, which is independent from other larger European loess. Therefore, it offers the possibility to study fine-scale variations in loess composition and deposition episodes. The five study sites were carefully chosen along the easternmost ridge of the Jura Mountains in order to highlight the main characteristics of Jura loess and propose an accurate and updated definition. The studied loess layers present similar compositions (grain-size distribution, mineralogical and geochemical compositions), thus indicating rather homogeneous loess, despite the identification of potential distinct aeolian episodes. The small dissimilarities observed between the profiles are partly linked to post-depositional pedogenesis. Indeed, Jura loess constitutes only thin deposits (<50 cm thick), which were influenced and modified by pedogenesis in their entire thickness. For example, the question of the primary calcite content in Jura loess is still unclear.

Observation of non-weathered Jura loess is made more difficult by the fact that loess particles were often reworked along hill slopes (e.g., in cover-beds) or incorporated into surficial layers of moraine deposits. Nevertheless, the presence of a loessic contribution is established in numerous soil profiles over the Jura Mountains and has obvious consequences on pedogenesis. In some places, a clear disconnection is observed between superficial deposits containing loess and the autochthonous weathering products or limestone bedrock (Martignier et al., 2013). Subsequently, the presence of an abundant silicate phase in the surface soil parent material can orientate pedogenesis towards unexpected acidic pathways in a carbonate environment (Martignier and Verrecchia, 2013).

Acknowledgements

This research was part of a M.Sc. thesis supported by the Universities of Lausanne and Neuchâtel, Switzerland. The authors would like to thank Dr. Luc Scherrer for his participation during the elaboration of the project and Jean-Claude Lavanchy (University of Lausanne) for performing geochemical analyses, as well as four reviewers who substantially improved the manuscript. This research has been partly supported by the GeoNova project (Swiss University Conference – CUS).

Appendix A. Supplementary data

Supplementary data associated with this article can be found, in the online version, at http://dx.doi.org/10.1016/j.aeolia.2015.05.003.

References

Adatte, T., Stinnesbeck, W., Keller, G., 1996. Lithostratigraphic and mineralogic correlations of near K/T boundary sediments in north-eastern Mexico: implications for origin and nature of deposition. In: Ryder, G., Fastovsky, D., Gartner, S. (Eds.), The Cretaceous-Tertiary Event and Other Catastrophes in Earth History. Geol. Soc. Am. Bull. (special paper), pp. 211–226.

Antoine, P., Rousseau, D.-D., Zöller, L., Lang, A., Munaut, A.-V., Hatté, C., Fontugne, M., 2001. High-resolution record of the last interglacial-glacial cycle in the Nussloch loess-palaeosol sequences, Upper Rhine Area, Germany. Quatern. Int. 76–77, 211–229.

Antoine, P., Rousseau, D.-D., Hatté, C., Zöller, L., Lang, A., Fontugne, M., Moine, O., 2002. Evénements éoliens rapides dans les Loess du Pléniglaciaire supérieur Weichselien: l'exemple de la séquence de Nussloch (vallée du Rhin-Allemagne). Quaternaire 13, 199–208.

Arn, R., Campy, M., 1990. Un problème de paléogéographie glaciaire au maximum würmien dans la zone circumalpine: le glacier jurassien. Bull. Soc. Neuchâtel. Sci. Nat. 113, 115–131.

Aubert, D., 1965. Calotte glaciaire et morphologie jurassiennes. Eclog. Geol. Helv. 58, 555–578.

Aubert, D., Gratier, M., Pochon, M., 1979. Livret-guide de quelques sols types du Haut-Jura et du pied du Jura. EPFL Péd. 4.

Campy, M., 1992. Palaeogeographical relationships between Alpine and Jura glaciers during the two last Pleistocene glaciations. Palaeogeogr. Palaeocl. 93, 1–12.

Cremaschi, M., 1990. The loess in Northern and Central Italy: A Loess Basin Between the Alps and the Mediterranean Region. CNR Centro di Studio per la Stratigrafia e la Petrografia delle Alpi Centrali, Milano.

Di Stefano, C., Ferro, V., Mirabile, S., 2010. Comparison between grain-size analyses using laser diffraction and sedimentation methods. Biosyst. Eng. 106, 205–215.

Duchaufour, P., 1983. Pédologie 1: Pédogenèse et classification. Masson, Paris.

FAO, 2006a. Guidelines for Soil Description. Food and Agriculture Organization of the United Nations (FAO), Rome.

FAO, 2006b. World Reference Base for Soil Resources 2006. Food and Agriculture Organization of the United Nations (FAO), Rome.

Ferraro, F., Terhorst, B., Ottner, F., Cremaschi, M., 2004. Val Sorda: an upper Pleistocene loess-paleosol sequence in northeastern Italy. Rev. Mex. Cienc. Geol. 21, 30–47.
Florineth, D., Schlüchter, C., 2000. Alpine evidence for atmospheric circulation patterns in Europe during the Last Glacial Maximum. Quat. Res. 54, 295–308.
Frechen, M., Oches, E.A., Kohfeld, K.E., 2003. Loess in Europe-mass accumulation rates during the Last Glacial Period. Quat. Sci. Rev. 22, 1835–1857.
Gillet, F., Havlicek, E., Rodaro, P., Gallandat, J.D., Ziliotto, U., 1996. Comparaison de quelques systèmes phytocénotiques de deux pâturages boisés des Dolomites d'Ampezzo (Italie). Diss. Bot. 258, 165–194.
Gratier, M., Bardet, L., 1980. Les sols du plateau vaudois. Mém. Soc. Vaud. Sci. Nat. 16, 89–188.
Guenat, C., 1987. Les sols forestiers non hydromorphes sur moraines du Jura vaudois (Ph.D. thesis). EPFL, Lausanne.
Haase, D., Fink, J., Haase, G., Ruske, R., Pécsi, M., Richter, H., Altermann, M., Jäger, K.D., 2007. Loess in Europe-its spatial distribution based on a European Loess Map, scale 1:2,500,000. Quat. Sci. Rev. 26, 1301–1312.
Hadorn, P., Thew, N., Russell Coope, G., Lemdahl, G., Hajdas, I., Bonani, G., 2002. A Late-Glacial and Early Holocene environment and climate history for the Neuchâtel region (CH). In: Richard, H., Vignot, A. (Eds.), Équilibres et Ruptures dans les Écosystemes Depuis 20 000 ans en Europe de l'Ouest. Presses Universitaires de Franche-Comté, Besançon, pp. 75–90.
Havlicek, E., 1999. Les sols des pâturages boisés du Jura suisse: origine et typologie, relations sol-végétation (Ph.D. thesis). University of Neuchâtel, Neuchâtel.
Havlicek, E., Gobat, J.M., 1996. Les apports éoliens dans les sols du Jura: état des connaissances et nouvelles données en pâturages boisés. Etude Gestion Sols 3, 167–178.
Havlicek, E., Gobat, J.M., Gillet, F., 1998. Réflexions sur les relations sol-végétation: trois exemples du Jura sur matériel allochtone. Ecologie 29, 535–546.
Ivy-Ochs, S., Schäfer, J., Kubik, P.W., Synal, H.A., Schlüchter, C., 2004. Timing of deglaciation on the northern Alpine foreland (Switzerland). Eclog. Geol. Helv. 97, 47–55.
Ivy-Ochs, S., Kerschner, H., Reuther, A., Preusser, F., Heine, K., Maisch, M., Kubik, P.W., Schlüchter, C., 2008. Chronology of the last glacial cycle in the European Alps. J. Quat. Sci. 23, 559–573.
Jamagne, M., 1973. Contribution à l'étude pédogénétique des formations loessiques du Nord de la France (Ph.D. thesis). INRA, Liège.
Kleber, A., 1992. Periglacial slope deposits and their pedogenic implications in Germany. Palaeogeogr. Palaeoclim. Palaeoecol. 99, 361–371.
Kleber, A., Terhorst, B., 2013. Mid-latitude slope deposits (cover-beds). Developments in Sedimentology 66. Elsevier, Amsterdam.
Kübler, B., Jantschik, R., Huon, S., 1990. Minéralogie et granulométrie des poussières éoliennes, dites "sahariennes", du 24 avril 1989 à Neuchâtel: leur importance pour l'environnement, les sols et les sédiments. Bull. Soc. Neuchâtel. Sci. Nat. 113, 75–98.
Lang, A., Hatté, C., Rousseau, D.-D., Antoine, P., Fontugne, M., Zöller, L., Hambach, U., 2003. High-resolution chronologies for loess: comparing AMS ^{14}C and optical dating results. Quat. Sci. Rev. 22, 953–959.
Lautridou, J.-P., 1984. Le cycle périglaciaire pléistocène en Europe du Nord-Ouest et plus particulièrement en Normandie (Ph.D. thesis). University of Caen, Caen.
Lorz, C., Heller, K., Kleber, A., 2011. Stratification of the regolith continuum – a key property for processes and functions of landscapes. Z. Geomorphol. 55, 277–292.
Luehmann, M.D., Schaetzl, R.J., Miller, B.A., Bigsby, M.E., 2013. Thin, pedoturbated, and locally sourced loess in the western Upper Peninsula of Michigan. Aeol. Res. 8, 85–100.
Magny, M., Thew, N., Hadorn, P., 2003. Late-glacial and early Holocene changes in vegetation and lake-level at Hauterive/Rouges-Terres, Lake Neuchâtel (Switzerland). J. Quat. Sci. 18, 31–40.
Mailänder, R., Veit, H., 2001. Periglacial cover-beds on the Swiss Plateau: indicators of soil, climate and landscape evolution during the Late Quaternary. Catena 45, 251–272.
Markovic, S.B., Oches, E., Sümegi, P., Jovanovic, M., Gaudenyi, T., 2006. An introduction to the Middle and Upper Pleistocene loess-paleosol sequence at Ruma brickyard, Vojvodina. Serb. Quatern. Int. 149, 80–86.
Martignier, L., 2013. Influence des formations superficielles sur l'évolution des sols du Jura Suisse (Ph.D. thesis). University of Lausanne, Lausanne.
Martignier, L., Verrecchia, E.P., 2013. Weathering processes in superficial deposits (regolith) and their influence on pedogenesis: a case study in the Swiss Jura Mountains. Geomorphology 189, 26–40.
Martignier, L., Adatte, T., Verrecchia, E.P., 2013. Bedrock versus superficial deposits in the Swiss Jura Mountains: what is the legitimate soil parent material? Earth Surf. Process. Landforms 38, 331–345.
Michalet, R., 1982. Influence du climat général sur l'évolution des sols à l'étage subalpin du Jura (Ph.D. thesis). University of Nancy I, Nancy.
Muhs, D.R., 2013. The geologic records of dust in the Quaternary. Aeol. Res. 9, 3–48.
Muhs, D.R., Budahn, J.R., 2006. Geochemical evidence for the origin of late Quaternary loess in central Alaska. Can. J. Earth Sci. 43, 323–337.
Muhs, D.R., Cattle, S.R., Crouvi, O., Rousseau, D.D., Sun, J., Zarate, M.A., 2014. Loess record. In: Knippertz, P., Stuut, J.B.W. (Eds.), Mineral Dust: A Key Player in the Earth System. Springer, p. 41.
Oinuma, K., Shimoda, S., Sudo, T., 1972. Triangular diagrams for surveying chemical compositions of chlorites. J. Tokio Univ., Gen. Edu. 15, 1–33.
Pochon, M., 1973. Apport allochtone dans les sols jurassiens (Jura vaudois et Jura neuchâtelois). Bull. Soc. Neuchâtel. Sci. Nat. 96, 135–147.
Pochon, M., 1978. Origine et évolution des sols du Haut-Jura suisse – phénomènes d'altération des roches calcaires sous climat tempéré humide (Ph.D. thesis). University of Neuchâtel, Neuchâtel.
Portmann, J.-P., 1954. Pétrographie des moraines du glacier würmien du Rhône dans la région des lacs subjurassiens (Suisse). Bull. Soc. Neuchâtel. Géogr. 5, 13–55.
Preusser, F., Fiebig, M., 2009. European middle Pleistocene loess chronostratigraphy: some considerations based on evidence from the Wels site. Aust. Quatern. Int. 198, 37–45.
Pye, K., 1987. Aeolian Dust and Dust Deposits. Academic Press, London.
Righi, D., Huber, K., Keller, C., 1999. Clay formation and Podzol development from postglacial moraines in Switzerland. Clay Miner. 34, 319–332.
Rousseau, D.D., Antoine, P., Hatté, C., Lang, A., Zöller, L., Fontugne, M., Othman, D.B., Luck, J.M., Moine, O., Labonne, M., Bentaleb, I., Jolly, D., 2002. Abrupt millennial climatic changes from Nussloch (Germany) Upper Weichselian eolian records during the Last Glaciation. Quat. Sci. Rev. 21, 1577–1582.
Schaetzl, R.J., Anderson, S., 2005. Soils: Genesis and Geomorphology. Cambridge University Press, Cambridge.
Schaetzl, R.J., Attig, J.W., 2013. The loess cover of northeastern Wisconsin. Quat. Res. 79, 199–214.
Schaetzl, R.J., Luehmann, M.D., 2013. Coarse-textured basal zones in thin loess deposits: Products of sediment mixing and/or paleoenvironmental change? Geoderma 192, 277–285.
Stanley, K.E., Schaetzl, R.J., 2011. Characteristics and paleoenvironmental significance of a thin, dual-sourced loess sheet, north-central Wisconsin. Aeol. Res. 2, 241–251.
Stuut, J.-B., Smalley, I., O'Hara-Dhand, K., 2009. Aeolian dust in Europe: African sources and European deposits. Quat. Int. 198, 234–245.
Terhorst, B., 2007. Periglacial cover beds and soils in landslide areas of SW-Germany. Catena 71, 467–476.
Terhorst, B., Damm, B., Peticzka, R., Köttritsch, E., 2009. Reconstruction of Quaternary landscape formation as a tool to understand present geomorphological processes in the eastern Prealps (Austria). Quat. Int. 209, 66–78.
Van Vliet-Lanoë, B., 2005. La Planète des Glaces, Histoire et Environnements de Notre ère Glaciaire. Vuibert, Paris.
Vandenberghe, J., 2013. Grain-size of fine-grained windblown sediment: a powerful proxy for process identification. Earth-Sci. Rev. 121, 18–30.
Velde, B., Meunier, A., 2008. The Origin of Clay Minerals in Soils and Weathered Rocks. Springer Verlag, Berlin.
Völkel, J., Leopold, M., Roberts, M.C., 2001. The radar signatures and ages of Periglacial slope deposits, Central Highlands of Germany. Permafrost Periglac. Process. 12, 379–387.
Völkel, J., Huber, J., Leopold, M., 2011. Significance of slope sediments layering on physical characteristics and interflow within the Critical Zone – examples from the Colorado Front Range, USA. Appl. Geochem. 26, S143–S145.
Zöller, L., Stremme, H., Wagner, G.A., 1988. Thermolumineszens-datierung an löss-Paläobodensequenzen von nieder-, mittel- und Oberrhein/Bundesrepublik Deutschland. Chem. Geol. 73, 39–62.